14

Blasius' viscous flow

Consider the two-dimensional laminar viscous flow past a semi-infinite flat plate, governed by

$$f'''(\eta) + \frac{1}{2} f(\eta) f''(\eta) = 0, \tag{14.1}$$

subject to the boundary conditions

$$f(0) = f'(0) = 0, \quad f'(+\infty) = 1, \tag{14.2}$$

where the prime denotes the derivative with respect to the similarity variable $\eta = y\sqrt{U_\infty/(\nu x)}$, the dimensionless function $f(\eta)$ is related to the stream function $\psi(x, y)$ by $f(\eta) = \psi/\sqrt{\nu x U_\infty}$, U_∞ is the constant velocity of the mainstream at infinity, ν is the kinematic viscosity coefficient, and x and y are two independent variables. For details, the reader is referred to White [20].

In 1908, Blasius [104] provided a solution in power series

$$f(\eta) = \sum_{k=0}^{+\infty} \left(-\frac{1}{2}\right)^k \frac{A_k \sigma^{k+1}}{(3k+2)!}\, \eta^{3k+2}, \tag{14.3}$$

where $\sigma = f''(0)$ and

$$A_0 = A_1 = 1, \qquad A_k = \sum_{r=0}^{k-1} \binom{3k-1}{3r} A_r\, A_{k-r-1} \quad (k \geq 2). \tag{14.4}$$

To get the unknown value of σ, Blasius [104] demonstrated another approximation of $f(\eta)$ for large η. Then, by means of matching two different approximations at a proper point, he obtained the numerical result $\sigma = 0.332$. In 1938, Howarth [105] gained a more accurate value $\sigma = 0.33206$ by means of a numerical technique. However, by means of $\sigma = 0.33206$, $f'(\eta)$ given by (14.3) is valid in a restricted region $0 \leq \eta < \rho_0$, where $\rho \approx 5.690$, as shown in Figure 14.1. Blasius' power series (14.3) is fundamentally an analytic-numerical solution, because the value of $\sigma = f''(0)$ is gained by numerical techniques.

In this chapter the homotopy analysis method is applied to yield the purely analytic solution expressions of Blasius' viscous flows by means of two different base functions.

14.1 Solution expressed by power functions

14.1.1 Zero-order deformation equation

Like Blasius [104], we express the solution of Equations (14.1) and (14.2) by the set of base functions

$$\left\{ \eta^{\alpha m+\beta} \quad | \quad m \geq 0 \right\} \tag{14.5}$$

in the form:

$$f(\eta) = \sum_{k=0}^{+\infty} a_k \, \eta^{\alpha k+\beta}, \tag{14.6}$$

where a_k is a coefficient, $\alpha > 0$ and $\beta \geq 0$ are constants. This provides us with the first *rule of solution expression* of Blasius' viscous flows.

Under the first *rule of solution expression* and using (14.2), it is easy to choose

$$f_0(\eta) = \frac{1}{2}\sigma\eta^2 \tag{14.7}$$

as the initial guess of $f(\eta)$, where $\sigma = f''(0)$. Then, under the first *rule of solution expression* denoted by (14.6) and from Equations (14.1) and (14.2), we choose the auxiliary linear operator

$$\mathcal{L}_0[\Phi(\eta;q)] = \frac{\partial^3\Phi(\eta;q)}{\partial\eta^3} \tag{14.8}$$

with the property

$$\mathcal{L}_0\left(C_0 + C_1\eta + C_2\eta^2\right) = 0, \tag{14.9}$$

where C_0, C_1, and C_2 are coefficients, $\Phi(\eta;q)$ is a real function of η and q, $q \in [0,1]$ is an embedding parameter. For brevity, we define from Equation (14.1) the nonlinear operator

$$\mathcal{N}[\Phi(\eta;q)] = \frac{\partial^3\Phi(\eta;q)}{\partial\eta^3} + \frac{1}{2}\Phi(\eta;q)\frac{\partial^2\Phi(\eta;q)}{\partial\eta^2}. \tag{14.10}$$

Let $\hbar$ denote a nonzero auxiliary parameter and $H(\eta)$ a nonzero auxiliary function. We construct the so-called zero-order deformation equation

$$(1-q)\,\mathcal{L}_0\left[\Phi(\eta;q) - f_0(\eta)\right] = q\,\hbar\,H(\eta)\,\mathcal{N}[\Phi(\eta;q)], \tag{14.11}$$

subject to the boundary conditions

$$\Phi(0;q) = 0, \left.\frac{\partial\Phi(\eta;q)}{\partial\eta}\right|_{\eta=0} = 0, \quad \left.\frac{\partial^2\Phi(\eta;q)}{\partial\eta^2}\right|_{\eta=0} = \sigma, \tag{14.12}$$

where $q \in [0,1]$ is an embedding parameter.

When $q = 0$, it is easy to demonstrate from (14.7), (14.11), and (14.12) that

$$\Phi(\eta; 0) = f_0(\eta). \tag{14.13}$$

When $q = 1$, since $\hbar \neq 0$ and $H(\eta) \neq 0$, the zero-order deformation equations (14.11) and (14.12) are equivalent to Equations (14.1) and (14.2), respectively, provided

$$\Phi(\eta; 1) = f(\eta). \tag{14.14}$$

As the embedding parameter q increases from 0 to 1, $\Phi(\eta; q)$ varies from the initial guess $f_0(\eta)$ to the exact solution $f(\eta)$.

Using Taylor's theorem and Equation (14.13), we expand $\Phi(\eta; q)$ in the power series

$$\Phi(\eta; q) = f_0(\eta) + \sum_{k=1}^{+\infty} f_k(\eta)\, q^k, \tag{14.15}$$

where

$$f_k(\eta) = \frac{1}{k!} \frac{\partial^k \Phi(\eta; q)}{\partial q^k}\bigg|_{q=0}. \tag{14.16}$$

Note that the zero-order deformation equation (14.11) contains the auxiliary parameter $\hbar$ and the auxiliary function $H(\eta)$. Assuming that both $\hbar$ and $H(\eta)$ are properly chosen so that the series (14.15) is convergent at $q = 1$, we have, using (14.14), that

$$f(\eta) = f_0(\eta) + \sum_{k=1}^{+\infty} f_k(\eta). \tag{14.17}$$

The mth-order approximation is given by

$$f(\eta) \approx f_0(\eta) + \sum_{k=1}^{m} f_k(\eta). \tag{14.18}$$

14.1.2 High-order deformation equation

For conciseness, define the vector

$$\vec{f}_n = \{f_0(\eta), f_1(\eta), f_2(\eta), \cdots, f_n(\eta)\}. \tag{14.19}$$

Differentiating the zeroth-order deformation equations (14.11) and (14.12) k times with respect to q, then setting $q = 0$, and finally dividing them by $k!$, we gain the high-order deformation equation

$$\mathcal{L}_0 \left[f_k(\eta) - \chi_k\, f_{k-1}(\eta)\right] = \hbar\, H(\eta)\, R_k(\vec{f}_{k-1}), \tag{14.20}$$

subject to the boundary conditions

$$f_k(0) = f_k'(0) = f_k''(0) = 0, \tag{14.21}$$

where χ_k is defined by (2.42) and

$$R_k(\vec{f}_{k-1}) = f'''_{k-1}(\eta) + \frac{1}{2}\sum_{n=0}^{k-1} f_n(\eta) f''_{k-1-n}(\eta). \tag{14.22}$$

Using (14.8), the solution of (14.20) is

$$\begin{aligned} f_k(\eta) = \chi_k f_{k-1}(\eta) + \hbar \int\int\int H(\eta)\, R_k(\vec{f}_{k-1})\, d\eta \\ + C_0 + C_1\eta + C_2\eta^2, \end{aligned} \tag{14.23}$$

where the coefficients C_0, C_1, and C_2 are determined by the boundary conditions (14.21), which then yields $f_k(\eta)$.

14.1.3 Convergence theorem

THEOREM 14.1
If the solution series (14.17) converges, where $f_k(\eta)$ is governed by Equations (14.20) and (14.21) under the definitions (14.22) and (2.42), it must be the solution of Equations (14.1) and (14.2).

Proof: From (2.42) and (14.20), we have

$$\hbar\, H(\eta) \sum_{k=1}^{m} R_k(\vec{f}_{k-1}) = \mathcal{L}[f_m(\eta)].$$

If the series (14.17) converges, then

$$\lim_{m\to+\infty} f_m(\eta) = 0.$$

Using (14.8), we have

$$\hbar\, H(\eta) \sum_{k=1}^{+\infty} R_k(\vec{f}_{k-1}) = \lim_{m\to+\infty} \mathcal{L}[f_m(\eta)] = \mathcal{L}\left[\lim_{m\to+\infty} f_m(\eta)\right] = 0,$$

which yields, since $\hbar \neq 0$ and $H(\eta) \neq 0$,

$$\sum_{k=1}^{+\infty} R_k(\vec{f}_{k-1}) = 0.$$

Substituting (14.22) into the above expression and simplifying it, we obtain

$$\frac{d^3}{d\eta^3}\left[\sum_{k=0}^{+\infty} f_k(\eta)\right] + \frac{1}{2}\left[\sum_{k=0}^{+\infty} f_k(\eta)\right]\frac{d^2}{d\eta^2}\left[\sum_{k=0}^{+\infty} f_k(\eta)\right] = 0.$$

From (14.7) and (14.21), we have

$$\sum_{k=0}^{+\infty} f_k(0) = \sum_{k=0}^{+\infty} f_k'(0) = 0, \quad \sum_{k=0}^{+\infty} f_k''(0) = \sigma.$$

Therefore, the solution series

$$f_0(\eta) + \sum_{k=1}^{+\infty} f_k(\eta)$$

must be the exact solution of Equations (14.1) and (14.2), as long as it is convergent. This ends the proof.

14.1.4 Result analysis

According to Theorem 14.1, we need only to focus on the convergence of the solution series (14.17) by properly choosing $\hbar$ and $H(\eta)$. Under the first *rule of solution expression* denoted by (14.6), the auxiliary function $H(\eta)$ takes the form

$$H(\eta) = \eta^{\kappa},$$

where κ is a constant. When $\kappa < 0$, the solution of Equations (14.20) and (14.21) contains the term

$$\eta \ln \eta,$$

which, however, disobeys the first *rule of solution expression* denoted by (14.6). We have therefore

$$\kappa \geq 0. \tag{14.24}$$

Note that there exist two auxiliary parameters: $\hbar$ and κ. We gain therefore a two-parameter family of solution expressions.

14.1.4.1 Solution expression when $H(\eta) = 1$

Consider the case of $\kappa = 0$, corresponding to $H(\eta) = 1$. In this case, Liao [28] found that the mth-order approximation (14.18) may be expressed by

$$f(\eta) \approx \sum_{k=0}^{m} \left[\left(-\frac{1}{2} \right)^k \frac{A_k \sigma^{k+1}}{(3k+2)!} \eta^{3k+2} \right] \mu_0^{m,k}(\hbar), \tag{14.25}$$

where $\mu_0^{m,k}(\hbar)$ is exactly the same as the expression (2.58) defined in Chapter 2 on page 22. We have the exact solution

$$f(\eta) = \lim_{m \to +\infty} \sum_{k=0}^{m} \left[\left(-\frac{1}{2} \right)^k \frac{A_k \sigma^{k+1}}{(3k+2)!} \eta^{3k+2} \right] \mu_0^{m,k}(\hbar). \tag{14.26}$$

The above expression provides us with a one-parameter family of solution expressions, although the solution of Equations (14.1) and (14.2) is unique. Note that $\mu_0^{m,k}(\hbar)$ appears once again. As proved in Chapter 2 on page 22,

$$\mu_0^{m,k}(-1) = 1.$$

Thus, when $\hbar = -1$, the solution series (14.26) is exactly the same as that of Blasius' one (14.3). Therefore, Blasius' solution (14.3) is a special case of (14.26). As pointed out by Liao [28], the solution (14.26) is valid in the region

$$\rho_0 \le \eta \le \rho_0 \left[\frac{2}{|\hbar|} - 1\right]^{1/3} \qquad (-2 < \hbar < 0), \tag{14.27}$$

where $\rho_0 \approx 5.690$ is the convergence radius of Blasius' power series (14.3). Thus, as $\hbar$ varies from -1 to 0, the convergence region of the solution series (14.26) enlarges from $\eta \in [-\rho_0, \rho_0]$ to $\eta \in [-\rho_0, +\infty)$, as shown in Figure 14.1. We are able to adjust and control the convergence region of the solution series (14.26) through use of the auxiliary parameter $\hbar$.

The power series (14.26) can be theoretically valid in the whole region $\eta \in [0, +\infty)$. Unlike Blasius [104], we do not need an additional solution for large η any more. Using the condition $f'(+\infty) = 1$, we can gain the value of $f''(0)$ by numerically solving the algebraic equation

$$\sum_{k=0}^{m} \left[\left(-\frac{1}{2}\right)^k \frac{A_k \sigma^{k+1}}{(3k+1)!}\, \eta_0^{3k+1}\right] \mu_0^{m,k}(\hbar) = 1 \tag{14.28}$$

for a proper value of $\hbar$ at a point $\eta = \eta_0$ far enough from $\eta = 0$. For a large enough order m of approximation and a small enough $\hbar$ ($-1 \le \hbar < 0$), the above equation at two points $\eta = 8$ and $\eta = 9$ gives the same value $\sigma = f''(0) = 0.33206$ that agrees with Howarth's numerical result [105], as shown in Table 14.1.

14.1.4.2 Solution expression when $H(\eta) = \eta$

Consider the case of $\kappa = 1$, corresponding to $H(\eta) = \eta$. Here, the mth-order approximation can be expressed by

$$f(\eta) \approx \frac{\sigma}{2}\,\eta^2 + \sum_{k=6}^{4m+2} b_{m,k}(\hbar)\,\eta^k, \tag{14.29}$$

where $b_{m,k}(\hbar)$ is a coefficient dependent of $\hbar$. Note that this solution does not contain the term η^5 and thus is different from the solution series (14.25). It also provides a new one-parameter family of solution expressions in $\hbar$. As $\hbar$ increases from -1 to 0, the convergence region of the solution series (14.29) enlarges, as shown in Figure 14.2. As $\hbar$ tends to 0 from below, the solution series (14.29) converges to the exact solution in the whole region $0 \le \eta < +\infty$ as in the solution series (14.25).

14.1.4.3 Solution expression when $H(\eta) = \sqrt{\eta}$

Consider the case of $\kappa = 1/2$, corresponding to $H(\eta) = \sqrt{\eta}$. Here, the mth-order approximation can be expressed by

$$f(\eta) \approx \frac{\sigma}{2}\,\eta^2 + \sum_{k=11}^{7m+4} c_{m,k}(\hbar)\,(\sqrt{\eta}\,)^k, \tag{14.30}$$

where $c_{m,k}(\hbar)$ is a coefficient dependent of $\hbar$. Note that this solution expression contains the term $\eta^{11/2}$ and thus is different from the solution series (14.25) and (14.29). It provides another one-parameter family of solution expressions in $\hbar$. As $\hbar$ increases from -1 to 0, the convergence region of the solution series (14.30) also enlarges, as shown in Figure 14.3. As $\hbar$ tends to 0 from below, the solution series (14.30) converges to the exact solution in the whole region $0 \le \eta < +\infty$, as in the series (14.25) and (14.29)

In general, for any given $\kappa \ge 0$, the corresponding solution series converges to the exact solution in the whole region $0 \le \eta < +\infty$ as $\hbar$ tends to zero from below. And, for given value of $\hbar$, the convergence region of the solution series given by $H(\eta) = 1$ appears to be the largest.

It should be emphasized that the solution series (14.29) and (14.30) are quite different from Blasius solution (14.3), which is a Taylor series. Note that, both (14.29) and (14.30) can converge in the whole region $0 \le \eta < +\infty$ and therefore are better than the Taylor series (14.3).

14.2 Solution expressed by exponentials and polynomials

14.2.1 Asymptotic property

Although the solution series (14.26), (14.29), and (14.30) given by power functions may be valid in the whole region $\eta \in [0, +\infty)$, as in Blasius' solution (14.3), it is still an analytic-numerical solution, because $\sigma = f''(0)$ had to be given by numerical techniques. Their convergence regions are dependent on $\hbar$, and when $|\hbar|$ is small, a large number of terms are needed to gain an accurate approximation for a large η. Therefore, they are not efficient solution expressions of Equations (14.1) and (14.2). This is mainly because the base functions defined by (14.5) do not automatically satisfy the boundary condition $f'(+\infty) = 1$ at infinity.

For very large η, Blasius [104] established from (14.1) and the boundary condition $f'(+\infty) = 1$ that

$$f'(\eta) \approx 1 + A \int \exp(-\eta^2/4) d\eta,$$

where A is an integral constant. Thus, $f(\eta) \to \eta$ exponentially as $\eta \to +\infty$. This is an important asymptotic property of $f(\eta)$. The velocity of the boundary layer physically tends to the mainstream velocity, exponentially.

To ensure that $f(\eta) \to \eta$ exponentially as $\eta \to +\infty$, we express $f(\eta)$ by the set of base functions

$$\{\eta, \eta^n \exp(-m\ \lambda\ \eta) \mid n \geq 0, m \geq 1, \lambda > 0\} \tag{14.31}$$

in the form:

$$f(\eta) = \eta + \sum_{m=1}^{+\infty} \sum_{n=0}^{+\infty} a_{m,n}\ \eta^n\ \exp(-m\ \lambda\ \eta), \tag{14.32}$$

where $\lambda > 0$ is the so-called spatial-scale parameter and $a_{m,n}$ is a coefficient. This provides us with the second *rule of solution expression* of Blasius viscous flow.

14.2.2 Zero-order deformation equation

According to the second *rule of solution expression* and using (14.2), it is easy to choose

$$\hat{f}_0(\eta) = \eta + \frac{1 - \exp(-\lambda\ \eta)}{\lambda} \tag{14.33}$$

as the initial guess of $f(\eta)$. Under the second *rule of solution expression* denoted by (14.32) and from Equations (14.1) and (14.2), we select the auxiliary linear operator

$$\hat{\mathcal{L}}[\Phi(\eta; q)] = \frac{\partial^3 \Phi(\eta; q)}{\partial \eta^3} + \lambda\ \frac{\partial^2 \Phi(\eta; q)}{\partial \eta^2} \tag{14.34}$$

with the property

$$\hat{\mathcal{L}}\left[C_0 + C_1 \eta + C_2 \exp(-\lambda\ \eta)\right] = 0, \tag{14.35}$$

where C_0, C_1, and C_2 are coefficients. Let $\hbar$ and $\hat{H}(\eta)$ denote a nonzero auxiliary parameter and a nonzero auxiliary function, respectively. Using the same definition $\mathcal{N}$ as (14.10), we construct the zero-order deformation equation

$$(1 - q)\ \hat{\mathcal{L}}\left[\hat{\Phi}(\eta; q) - \hat{f}_0(\eta)\right] = q\ \hbar\ \hat{H}(\tau)\ \mathcal{N}[\hat{\Phi}(\eta; q)], \tag{14.36}$$

subject to the boundary conditions

$$\hat{\Phi}(0; q) = 0, \quad \left.\frac{\partial \hat{\Phi}(\eta; q)}{\partial \eta}\right|_{\eta=0} = 0, \quad \left.\frac{\partial \hat{\Phi}(\eta; q)}{\partial \eta}\right|_{\eta=+\infty} = 1, \tag{14.37}$$

where $q \in [0, 1]$ is an embedding parameter, $\hat{\Phi}(\eta; q)$ is a real function of η and q.

As shown in §14.1.1, we have the relationship

$$f(\eta) = \hat{f}_0(\eta) + \sum_{k=1}^{+\infty} \hat{f}_k(\eta), \tag{14.38}$$

where

$$\hat{f}_k(\eta) = \frac{1}{k!} \frac{\partial^k \hat{\Phi}(\eta; q)}{\partial q^k}\bigg|_{q=0}. \tag{14.39}$$

14.2.3 High-order deformation equation

Define the vector

$$\mathbf{f}_n = \left\{ \hat{f}_0(\eta), \hat{f}_1(\eta), \hat{f}_2(\eta), \cdots, \hat{f}_n(\eta) \right\}.$$

Similarly, differentiating the zero-order deformation equations (14.36) and (14.37) k times with respect q, then setting $q = 0$, and finally dividing by $k!$, we have the high-order deformation equation

$$\hat{\mathcal{L}} \left[\hat{f}_k(\eta) - \chi_k \hat{f}_{k-1}(\eta) \right] = \hbar \, \hat{H}(\eta) \, \hat{R}_k(\mathbf{f}_{k-1}), \tag{14.40}$$

subject to the boundary conditions

$$\hat{f}_k(0) = \hat{f}'_k(0) = \hat{f}'_k(+\infty) = 0, \tag{14.41}$$

where χ_k is defined by (2.42) and

$$\hat{R}_k(\mathbf{f}_{k-1}) = \hat{f}'''_{k-1}(\eta) + \frac{1}{2} \sum_{n=0}^{k-1} \hat{f}_n(\eta) \, \hat{f}''_{k-1-n}(\eta). \tag{14.42}$$

14.2.4 Recursive expressions

Considering the wide applications of Blasius' viscous flows, it is helpful to express its solution explicitly. Under the second *rule of solution expression* denoted by (14.32), the auxiliary function $\hat{H}(\eta)$ may be in the form

$$\hat{H}(\eta) = \eta^m \, \exp(-\lambda \, n \, \eta), \qquad m \geq 0, \quad n \geq 0.$$

For simplicity, we select

$$\hat{H}(\eta) = 1. \tag{14.43}$$

Thereafter, by solving the first several high-order deformation equations (14.40) and (14.41), $\hat{f}_m(\eta)$ can be expressed by

$$\hat{f}_m(\eta) = b_0^{m,0} + \sum_{n=1}^{m+1} \exp(-n\lambda \, \eta) \sum_{k=0}^{2(m+1-n)} b_k^{m,n} \, \eta^k, \tag{14.44}$$

where $b_k^{m,n}$ is a coefficient. Substituting this expression into Equations (14.40) and (14.41), we obtain the following recurrence formulae

$$
\begin{aligned}
b_0^{m,0} &= \chi_m b_0^{m-1,0} - \lambda^{-1} \sum_{r=0}^{2m-1} \Gamma_r^{m,1}\Pi_r^{1,1} - \sum_{n=2}^{m+1}(n-1)\Gamma_0^{m,n}\Pi_0^{n,0} \\
&\quad + \sum_{n=2}^{m+1} \sum_{r=1}^{2(m-n+1)} \Gamma_r^{m,n}\left(n\Pi_r^{n,0} - \Pi_r^{n,0} - \lambda^{-1}\Pi_r^{n,1}\right), \\
b_0^{m,1} &= \chi_m b_0^{m-1,1} + \lambda^{-1} \sum_{r=0}^{2m-1} \Gamma_r^{m,1}\Pi_r^{1,1} \\
&\quad + \sum_{n=2}^{m+1} \left[n\Gamma_0^{m,n}\Pi_0^{n,0} + \sum_{r=1}^{2(m-n+1)} \Gamma_r^{m,n}\left(n\Pi_r^{n,0} - \lambda^{-1}\Pi_r^{n,1}\right) \right], \\
b_k^{m,1} &= \chi_m(1-\chi_{k+3-2m}) b_k^{m-1,1} + \sum_{r=k-1}^{2m-1} \Gamma_r^{m,1}\Pi_r^{1,k} \qquad (1 \le k \le 2m), \\
b_k^{m,n} &= \chi_m(1-\chi_{k+1-2m+2n}) b_k^{m-1,n} - \sum_{r=k}^{2(m-n+1)} \Gamma_r^{m,n}\Pi_r^{n,k} \\
&\qquad (2 \le n \le m, 0 \le k \le 2m-2n+2)
\end{aligned}
$$

and

$$b_0^{m,m+1} = -\Gamma_0^{m,m+1}\Pi_0^{m+1,0},$$

where

$$
\begin{aligned}
\Pi_r^{1,k} &= \frac{r!\,(r-k+2)}{k!\,\lambda^{r-k+3}} (0 \le k \le r+1), \\
\Pi_r^{n,k} &= \frac{r!}{k!(n-1)^{r-k+1}\lambda^{r-k+3}} \left[1 - \left(1 - \frac{1}{n}\right)^{r-k+1} \left(1 + \frac{r-k+1}{n}\right) \right] \\
&\qquad (n \ge 2, 0 \le k \le r),
\end{aligned}
$$

$$
\begin{aligned}
\Gamma_r^{m,n} &= \hbar\left[(1-\chi_{r+1-2m+2n})\, d_r^{m-1,n} + \delta_r^{m,n}\right] \\
&\qquad (1 \le n \le m, 0 \le r \le 2m-2n+2),
\end{aligned}
$$

in which

$$
\begin{aligned}
\delta_r^{m,n} = \frac{1}{2} \sum_{k=0}^{m-1} & \sum_{j=\max\{1,n+k-m\}}^{\min\{n,k+1\}} \sum_{i=\max\{0,r-2(m-k-n+j)\}}^{\min\{r,2(k-j+1)\}} \\
& \times c_i^{k,j}\; b_{r-i}^{m-1-k,n-j}\; \Lambda_{r-i}^{m-1-k,n-j}
\end{aligned}
$$

under the definitions

$$c_n^{m,k} = (n+1)(n+2)(1-\chi_{n+1-2m+2k})\, b_{n+2}^{m,k} \\ -2(k\lambda)(n+1)(1-\chi_{n-2m+2k})\, b_{n+1}^{m,k} + (k\lambda)^2\, b_n^{m,k},$$

$$d_n^{m,k} = (n+1)(1-\chi_{n-2m+2k})\, c_{n+1}^{m,k} - k\lambda c_n^{m,k}$$

and

$$\Lambda_k^{i,j} = \begin{cases} 0, \text{ when } i=j=0, k\geq 2, \\ 0, \text{ when } i>0, j=0, k\geq 1, \\ 0, \text{ when } j>i+1, \\ 0, \text{ when } k>2(i+1-j), \\ 1, \text{ otherwise.} \end{cases} \tag{14.45}$$

Using (14.33), we gain the first three coefficients

$$b_0^{0,0} = -\lambda^{-1}, \quad b_1^{0,0} = 1, \quad b_0^{0,1} = \lambda^{-1}. \tag{14.46}$$

From these three coefficients and using the above recurrence formulae, we can calculate all coefficients $b_k^{m,n}$. For details, the reader is referred to Liao [29].

Substituting (14.44) into (14.38), we obtain the solution

$$f(\eta) = \eta \\ + \lim_{M\to+\infty}\left[\sum_{m=0}^{M} b_0^{m,0} + \sum_{n=1}^{M+1}\exp(-n\lambda\,\eta)\left(\sum_{m=n-1}^{M}\sum_{k=0}^{2(m-n+1)} b_k^{m,n}\,\eta^k\right)\right]. \tag{14.47}$$

Note that the coefficient $b_k^{m,n}$ contains the auxiliary parameter $\hbar$ and the so-called spatial-scale parameter λ. It provides us with a two-parameter family of solution expressions. Note that the solution series (14.47) is explicit and has the asymptotic property $f'(\eta)\to 1$ exponentially as $\eta\to+\infty$.

14.2.5 Convergence theorem

THEOREM 14.2

If the solution series (14.38) converges, where $\hat{f}_k(\eta)$ is governed by Equations (14.40) and (14.41) under the definitions (14.42) and (2.42), it must be the solution of Equations (14.1) and (14.2).

Proof: From (2.42) and (14.40), it holds that

$$\hbar\,\hat{H}(\eta)\sum_{k=1}^{m}\hat{R}_k(\mathbf{f}_{k-1}) = \hat{\mathcal{L}}\,[\hat{f}_m(\eta)].$$

If the series (14.38) converges, it is necessary that

$$\lim_{m\to+\infty} \hat{f}_m(\eta) = 0.$$

Then, using (14.34), we have

$$\hbar\, \hat{H}(\eta) \sum_{k=1}^{+\infty} \hat{R}_k(\mathbf{f}_{k-1}) = \lim_{m\to+\infty} \hat{\mathcal{L}}[\hat{f}_m(\eta)] = \hat{\mathcal{L}}\left[\lim_{m\to+\infty} \hat{f}_m(\eta)\right] = 0,$$

which gives, since $\hbar \neq 0$ and $\hat{H}(\eta) \neq 0$,

$$\sum_{k=1}^{+\infty} \hat{R}_k(\mathbf{f}_{k-1}) = 0.$$

Substituting (14.42) into the above expression and simplifying it, we obtain

$$\frac{d^3}{d\eta^3}\left[\sum_{k=0}^{+\infty} \hat{f}_k(\eta)\right] + \frac{1}{2}\left[\sum_{k=0}^{+\infty} \hat{f}_k(\eta)\right] \frac{d^2}{d\eta^2}\left[\sum_{k=0}^{+\infty} \hat{f}_k(\eta)\right] = 0.$$

From (14.33) and (14.41),

$$\sum_{k=0}^{+\infty} \hat{f}_k(0) = \sum_{k=0}^{+\infty} \hat{f}'_k(0) = 0, \quad \sum_{k=0}^{+\infty} \hat{f}_k(+\infty) = 1.$$

Therefore, the series

$$\hat{f}_0(\eta) + \sum_{k=1}^{+\infty} \hat{f}_k(\eta)$$

must be the exact solution of Equations (14.1) and (14.2) as long as it is convergent. This ends the proof.

14.2.6 Result analysis

According to Theorem 14.2, we need only to focus on correctly choosing the auxiliary parameter $\hbar$ and the spatial-scale parameter λ so that the solution series (14.47) is convergent. For simplicity, we consider first the convergence of $f''(0)$ that is dependent on $\hbar$ and λ. We first set $\hbar = -1$ and regard λ as an unknown variable. For large enough λ such as $\lambda \geq 4$, the approximation of $f''(0)$ converges to the same value, as shown in Figure 14.4. In general, for given $\lambda \geq 4$, we investigate the influence of $\hbar$ on the convergence of the solution series (14.47) using the so-called $\hbar$-curves (see page 26 and §3.5.1) of $f''(0)$. For example, the $\hbar$-curves of $f''(0)$ when $\lambda = 4$ clearly indicate that the valid region of $\hbar$ is $-3/2 \leq \hbar \leq -1/2$, as shown in Figure 14.5. For instance, when $\lambda = 4$ and $\hbar = -1$, the approximation sequence of $f''(0)$ given by

(14.47) converges to 0.332057, which agrees with Howarth's [105] numerical result $f''(0) = 0.33206$, as shown in Table 14.2. The larger the absolute value of $\hbar$, the faster the sequence of $f''(0)$ converges. When $\hbar = -3/2$ and $\lambda = 4$, we obtain the accurate result $f''(0) = 0.332057$ at the 25th-order of approximation.

The homotopy-Padé technique (see page 38 and §3.5.2) can be applied to accelerate the convergence of $f''(0)$, as shown in Table 14.3. It is found that the $[m, m]$ homotopy-Padé approximants of $f''(0)$ do not depend upon the auxiliary parameter $\hbar$. Besides, the convergence rate of the $[m, m]$ homotopy-Padé approximants of $f''(0)$ is not sensitive to λ, as shown in Table 14.4. From Figure 14.4, it is clear that $f''(0)$ is divergent when $\hbar = -1$ and $\lambda \leq 2$. When $\lambda = 2$ and $\hbar = -1$, the 30th-order approximation of $f''(0)$ is equal to -3.7×10^9. However, even when $\lambda \leq 2$ such as $\lambda = 1$ and $\lambda = 2$, the sequence of the homotopy-Padé approximants of $f''(0)$ still converges to 0.332057, as shown in Table 14.4. We see that, the $[m, m]$ homotopy-Padé approximant of $f''(0)$ is not only independent of the auxiliary parameter $\hbar$ but also insensitive to the auxiliary parameter λ.

As long as the sequence of $f''(0)$ is convergent, the corresponding solution series of $f(\eta)$ and $f'(\eta)$ also converges to Howarth's [105] numerical result in the whole region $0 \leq \eta < +\infty$. For example, when $\lambda = 4$ and $\hbar = -1$, $f'(\eta)$ converges to Howarth's [105] numerical result in the whole region $0 \leq \eta < +\infty$, as shown in Table 14.5. Similarly, we can apply the homotopy-Padé technique to accelerate the convergence rate of the series (14.47); the $[m, m]$ homotopy-Padé approximants of $f(\eta)$ and $f'(\eta)$ are independent of $\hbar$. As mentioned before, the approximation sequence of $f''(0)$ diverges when $\lambda = 2$ and $\hbar = -1$. However, by means of the Homotopy-Padé technique, we obtain convergent results of $f(\eta)$ in the whole region $0 \leq \eta < +\infty$ even when $\lambda = 2$ and $\hbar = -1$, as shown in Table 14.6. When $\lambda = 2$ and $\hbar = -1$, even the [5,5] homotopy-Padé approximant of $f'(\eta)$ is accurate enough, as shown in Figure 14.6.

Note that the solution (14.47) is explicit, purely analytic, and uniformly valid in the *whole* region $\eta \in [0, +\infty)$. Thus, it can be regarded as a definition of the solution of Blasius' viscous flow problems governed by Equations (14.1) and (14.2).

This example demonstrates once again that, using the homotopy analysis method, we can obtain many different solution expressions of a nonlinear problem, even if the solution is unique.

TABLE 14.1
Numerical values of $f''(0)$ given by (14.28) for different $\hbar, \eta_0$, and the order m of approximation.

m	$\hbar = -\frac{1}{10}$ and $\eta_0 = 8$	$\hbar = -\frac{1}{12}$ and $\eta_0 = 9$
20	0.32881	0.32743
40	0.33185	0.33149
60	0.33205	0.33201
80	0.33206	0.33205
90	0.33206	0.33206
100	0.33206	0.33206

Source: reprinted from *International Journal of Non-Linear Mechanics*, 32, Shi-Jun Liao, "A kind of approximate solution technique which does not depend upon small parameters (II): An application in fluid mechanics", 815-822, Copyright (1997), with permission from Elsevier.

TABLE 14.2
Analytic approximations of $f''(0)$ given by (14.47) when $\hbar = -1$ and $\lambda = 4$.

Order of approximation	$f''(0)$
10th	0.327756
20th	0.331851
30th	0.332040
40th	0.332055
45th	0.332057
50th	0.332057
55th	0.332057

Source: Shi-Jun Liao, "A uniformly valid analytic solution of two-dimensional viscous flow past a semi-infinite flat plate", *Journal of Fluid Mechanics* (1999), 385:101-128 Cambridge University Press Copyright ©1999 Cambridge University Press, reprinted with permission.

TABLE 14.3
The $[m, m]$ homotopy-Padé approximation of $f''(0)$ when $\hbar = -1$ and $\lambda = 4$.

$[m, m]$	homotopy-Padé approximant of $f''(0)$
$[4, 4]$	0.344675
$[8, 8]$	0.332055
$[12, 12]$	0.332056
$[16, 16]$	0.332057
$[20, 20]$	0.332057
$[25, 25]$	0.332057

TABLE 14.4
The $[m, m]$ homotopy-Padé approximation of $f''(0)$ for different values of λ.

$[m, m]$	$\lambda = 1$	$\lambda = 2$	$\lambda = 4$	$\lambda = 5$	$\lambda = 10$
$[4, 4]$	0.326857	0.331867	0.344675	0.362964	0.519751
$[8, 8]$	0.331808	0.331753	0.332055	0.332269	0.347726
$[12, 12]$	0.332008	0.332056	0.332056	0.332053	0.332908
$[16, 16]$	0.332043	0.332057	0.332057	0.332057	0.332084
$[20, 20]$	0.332054	0.332057	0.332057	0.332057	0.332057
$[25, 25]$	0.332057	0.332057	0.332057	0.332057	0.332057

TABLE 14.5
Comparison of Howarth's [105] numerical results of $f'(\eta)$ with the analytic approximations given by (14.47) when $\hbar = -1$ and $\lambda = 4$.

η	20th order	30th order	40th order	50th order	55th order	numerical result
0.4	0.132650	0.132756	0.132763	0.132764	0.132764	0.1328
0.8	0.264412	0.264488	0.264707	0.264709	0.264709	0.2647
1.2	0.393075	0.393755	0.393772	0.393776	0.393776	0.3938
1.6	0.514758	0.516680	0.516750	0.516756	0.516756	0.5168
2.0	0.626372	0.629553	0.629754	0.629764	0.629764	0.6298
2.4	0.727156	0.728494	0.728950	0.728980	0.728980	0.7290
2.8	0.814839	0.810980	0.811429	0.811503	0.811503	0.8115
3.2	0.885026	0.876124	0.875982	0.876066	0.876066	0.8761
3.6	0.935172	0.924321	0.923315	0.923312	0.923312	0.9233
4.0	0.966854	0.957245	0.955665	0.955518	0.955518	0.9555
4.4	0.984622	0.977780	0.976154	0.975900	0.975900	0.9759
5.0	0.995914	0.992920	0.991856	0.991599	0.991599	0.9916
6.0	0.999708	0.999317	0.999092	0.999006	0.999006	0.9990
7.0	0.999987	0.999961	0.999939	0.999926	0.999926	1.0000
8.0	1.000000	0.999999	0.999998	0.999997	0.999997	1.0000

Source: Shi-Jun Liao, "A uniformly valid analytic solution of two-dimensional viscous flow past a semi-infinite flat plate", *Journal of Fluid Mechanics* (1999), 385:101-128 Cambridge University Press Copyright ©1999 Cambridge University Press, reprinted with permission.

TABLE 14.6
Comparison of Howarth's [105] numerical results with the $[m, m]$ homotopy-Padé approximation of $f'(\eta)$ when $\lambda = 2$ and $\hbar = -1$.

η	$[5, 5]$	$[10, 10]$	$[15, 15]$	$[20, 20]$	$[25, 25]$	numerical result
0.4	0.133023	0.132814	0.132764	0.132764	0.132764	0.1328
0.8	0.264655	0.264688	0.264709	0.264709	0.264709	0.2647
1.2	0.393380	0.393774	0.393775	0.393776	0.393776	0.3938
1.6	0.516251	0.516751	0.516755	0.516757	0.516757	0.5168
2.0	0.629577	0.629759	0.629765	0.629766	0.629766	0.6298
2.4	0.729388	0.728968	0.728981	0.728982	0.728982	0.7290
2.8	0.812514	0.811489	0.811508	0.811509	0.811510	0.8115
3.2	0.877471	0.876059	0.876079	0.876081	0.876081	0.8761
3.6	0.924790	0.923298	0.923325	0.923329	0.923330	0.9233
4.0	0.956803	0.955468	0.955523	0.955518	0.955518	0.9555
4.4	0.976987	0.975798	0.975872	0.975871	0.975870	0.9759
5.0	0.992848	0.991460	0.991542	0.991542	0.991542	0.9916
6.0	1.000400	0.998920	0.998972	0.998974	0.998973	0.9990
7.0	0.999989	0.999920	0.999920	0.999922	0.999921	1.0000
8.0	0.999998	0.999995	0.999996	0.999997	0.999996	1.0000

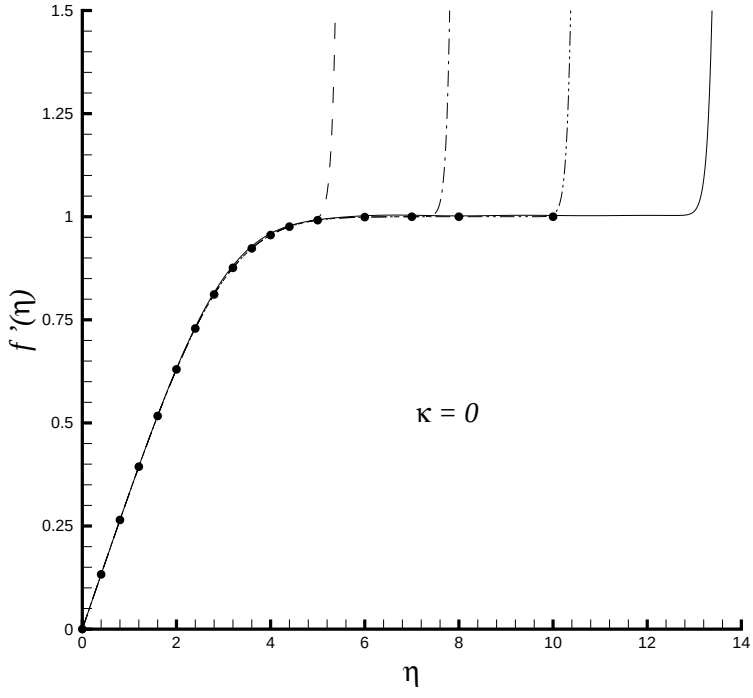

FIGURE 14.1
Comparison of Howarth's [105] numerical result of $f''(0)$ with the solution series (14.26) when $H(\eta) = 1$ by means of different values of $\hbar$. Symbols: numerical result; dashed line: $\hbar = -1$ (Blasius' power series); dash-dotted line: $\hbar = -1/2$; dash-dot-dotted line: $\hbar = -1/4$; solid line: $\hbar = -1/8$.

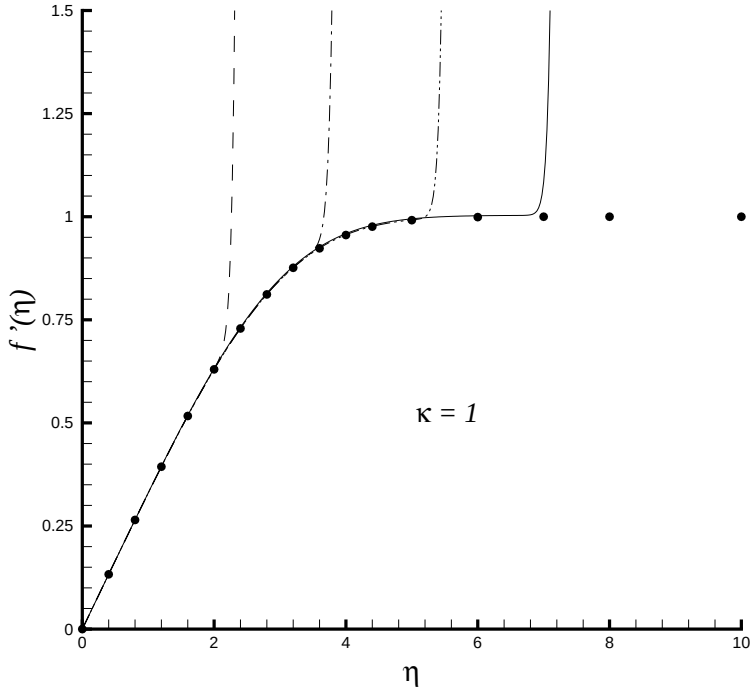

FIGURE 14.2
Comparison of Howarth's [105] numerical result of $f''(0)$ with the solution series (14.29) when $H(\eta) = \eta$ by means of different values of $\hbar$. Symbols: numerical result; dashed line: $\hbar = -1$ (Blasius' power series); dash-dotted line: $\hbar = -1/2$; dash-dot-dotted line: $\hbar = -1/4$; solid line: $\hbar = -1/8$.

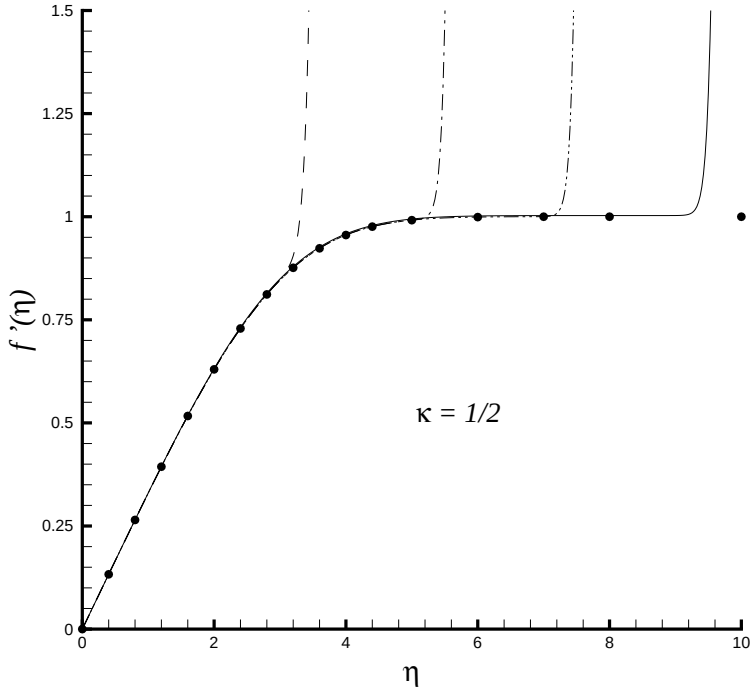

FIGURE 14.3
Comparison of Howarth's [105] numerical result of $f''(0)$ with the solution series (14.30) when $H(\eta) = \sqrt{\eta}$ by means of different values of $\hbar$. Symbols: numerical result; dashed line: $\hbar = -1$ (Blasius' power series); dash-dotted line: $\hbar = -1/2$; dash-dot-dotted line: $\hbar = -1/4$; solid line: $\hbar = -1/8$.

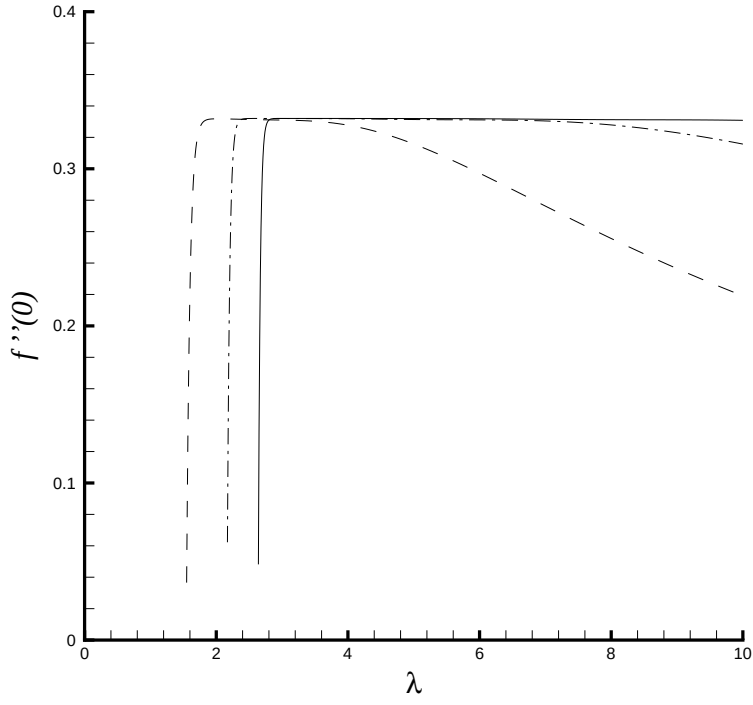

FIGURE 14.4
$f''(0)$ given by (14.47) for different λ when $\hbar = -1$. Dashed line: 10th-order approximation; dash-dotted line: 20th-order approximation; solid line: 30th-order approximation.

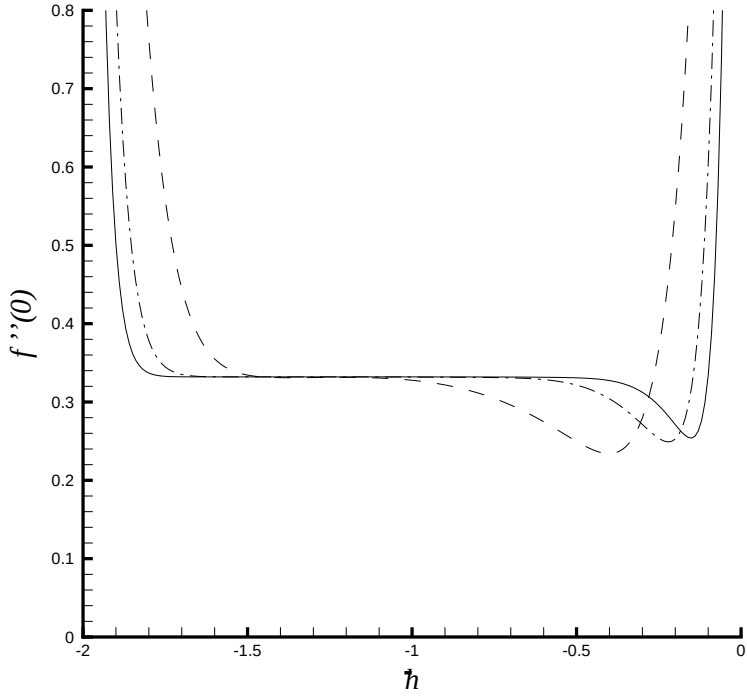

FIGURE 14.5
The $\hbar$-curves of $f''(0)$ given by (14.47) when $\lambda = 4$. Dashed line: 10th-order approximation; dash-dotted line: 20th-order approximation; solid line: 30th-order approximation.

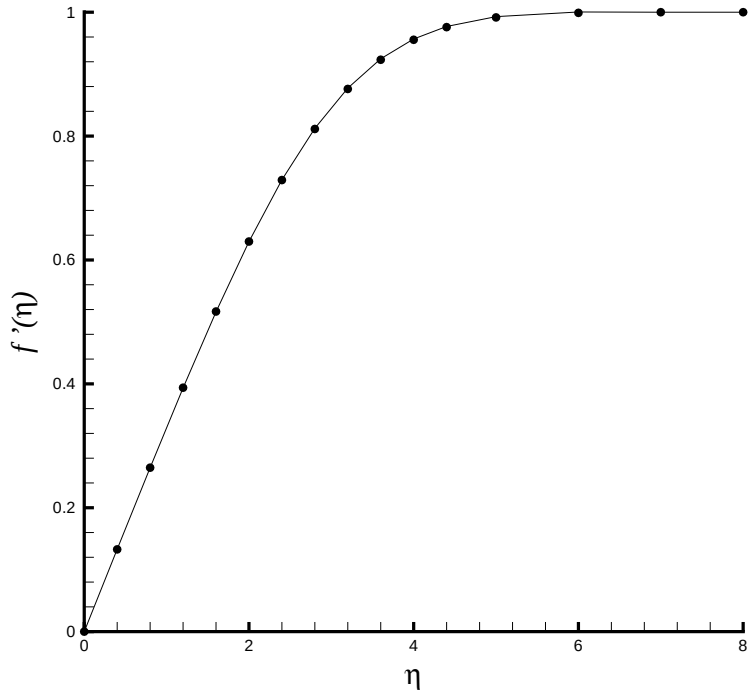

FIGURE 14.6
Comparison of Howarth's [105] numerical result of $f'(\eta)$ with the [5,5] homotopy-Padé approximation when $\lambda = 2$ and $\hbar = -1$. Symbols: numerical result; solid line: [5,5] homotopy-Padé approximation.